Correlation between the Microscopic Morphology and the Solid-State Photoluminescence Properties in Fluorene-Based Polymers and Copolymers

Mathieu Surin,[†] Emmanuelle Hennebicq,[†] Christophe Ego,[‡] Dirk Marsitzky,[‡] Andrew C. Grimsdale,[‡] Klaus Müllen,[‡] Jean-Luc Brédas,[†,§] Roberto Lazzaroni,*[,†] and Philippe Leclère[†]

Service de Chimie des Matériaux Nouveaux, Centre de Recherche en Electronique et Photonique Moléculaires, Université de Mons-Hainaut, Place du Parc 20, B-7000 Mons, Belgium, Max-Planck-Institut für Polymerforschung, Ackermannweg 10, D-55128 Mainz, Germany, and School of Chemistry and Biochemistry, Georgia Institute of Technology, Atlanta, Georgia 30332-0400

Received October 2, 2003. Revised Manuscript Received January 16, 2004

The microscopic morphology of a series of substituted fluorene-based conjugated polymers and copolymers are analyzed with tapping-mode atomic force microscopy. Different structures are observed depending on the nature of the substituents. Thin deposits of polyfluorenes substituted with linear alkyl groups are made of long fibrils, with lateral dimensions on the order of a few nanometers; polymers with branched alkyl or aromatic substituents form homogeneous, featureless films. To understand how polymer chains pack into these structures, comparisons are made with molecular modeling calculations; the simulation results highlight the dependence between intermolecular $\pi-\pi$ interactions and steric hindrance among substituents: linear alkyl substituents allow for a close packing of the conjugated chains into very long, regular $\pi-\pi$ stacks, in contrast to the bulkier substituents. A strong correlation is established between the degree of order in the thin deposits and the solid-state photoluminescence spectra; a red shift and the formation of a broad emission band in the green region are observed for deposits showing long-range organization, which is attributed to the formation of aggregates of well-organized, densely packed molecules.

Introduction

Conjugated polymers and oligomers offer new opportunities in information technology since they can be used as active materials in light-emitting diodes,[1,2] field-effect transistors,[3−5] and plastic solar cells.[6] In the case of light-emitting diodes (LEDs), stable blue-emitting materials are needed to fabricate full-color devices and poly(*p*-phenylene) (PPP)[7] and related polymers, such as ladder-type PPP, polyfluorenes, and polyindenofluorenes, have attracted strong interest in recent years.[8−10] Polyfluorenes (PFs, Scheme 1) are especially good candidates for LED applications because of their high solid-state photoluminescence (PL) quantum efficiencies, excellent solubility and film-forming capability, and the ease in controlling their properties via facile substitution in the 9-position (the bridging site).[9,11−14] Much effort has been devoted to tuning the optoelectronic properties of PFs through macromolecular engineering: for example, specific substituents or end groups have been used to improve solubility, create cross-linkable polymers, and modulate the optical and charge injection properties;[15−19] copolymers of fluorene with

* To whom correspondence should be addressed.
† Université de Mons-Hainaut.
‡ Max-Planck-Institut für Polymerforschung.
§ Georgia Institute of Technology.

(1) Kraft, A.; Grimsdale, A. C.; Holmes, A. B. *Angew. Chem., Int. Ed.* **1998**, *37*, 402.
(2) Friend, R. H.; Gymer, R. W.; Holmes, A. B.; Burroughes, J. H.; Marks, R. N.; Taliani, C.; Bradley, D. D. C.; dos Santos, D. A.; Brédas, J. L.; Lögdlund, M.; Salaneck, W. R. *Nature* **1999**, *397*, 121.
(3) Garnier, F.; Hajlaoui, R.; Yassar, A.; Srivastava, P. *Science* **1994**, *265*, 1684.
(4) Lin, Y.-Y.; Gundlach, D. J.; Nelson, S. F.; Jackson, T. N. *IEEE Trans. Electron Devices* **1997**, *44*, 1325.
(5) Horowitz, G. *Adv. Mater.* **1998**, *10*, 365.
(6) Brabec, C. J.; Sariciftci, N. S.; Hummelen, J. C. *Adv. Funct. Mater.* **2001**, *11*, 15.
(7) Grem, G.; Leditzky, G.; Ullrich, B.; Leising, G. *Adv. Mater.* **1992**, *4*, 36.
(8) Huber, J.; Müllen, K.; Salbeck J.; Schenk, H.; Scherf, U.; Stehlin, T.; Stern, R. *Acta Polym.* **1994**, *45*, 244.
(9) Grice, A. W.; Bradley, D. D. C.; Bernius, M. T.; Inbasekaran, M.; Wu, W. W.; Woo, E. P. *Appl. Phys. Lett.* **1998**, *73*, 629.
(10) Setayesh, S.; Marsitzky, D.; Müllen, K. *Macromolecules* **2000**, *33*, 2016.
(11) Bernius, M. T.; Inbasekaran, M.; O'Brien, J.; Wu, W. S. *Adv. Mater.* **2000**, *12*, 1737.
(12) Neher, D. *Macromol. Rapid Commun.* **2001**, *22*, 1365.
(13) Scherf, U.; List, E. W. J. *Adv. Mater.* **2002**, *14*, 477.
(14) Leclerc, M. *J. Polym. Sci., Part A: Polym. Chem.* **2001**, *39*, 2867.
(15) Pei, Q.; Yang, Y. *J. Am. Chem. Soc.* **1996**, *118*, 7416.
(16) Klärner, G.; Lee, J.-I.; Chan, E.; Chen, J.-P.; Nelson, A.; Marckiewicz, D.; Siemens, R.; Scott, J. C.; Miller, R. D. *Chem. Mater.* **1999**, *11*, 1800.
(17) Setayesh, S.; Grimsdale, A. C.; Weil, T.; Enkelmann, V.; Müllen, K.; Meghdadi, F.; List, E. J. W.; Leising, G. *J. Am. Chem. Soc.* **2001**, *123*, 946.
(18) Miteva, T.; Meisel, A.; Knoll, W.; Nothofer, H. G.; Scherf, U.; Müller, D. C.; Meerholz, K.; Yasuda, A.; Neher, D. *Adv. Mater.* **2001**, *13*, 565.
(19) Ego, C.; Grimsdale, A. C.; Uckert, F.; Yu, G.; Srdanov, G.; Müllen, K. *Adv. Mater.* **2002**, *14*, 809.

10.1021/cm0349452 CCC: $27.50
Published on Web 02/14/2004

Scheme 1

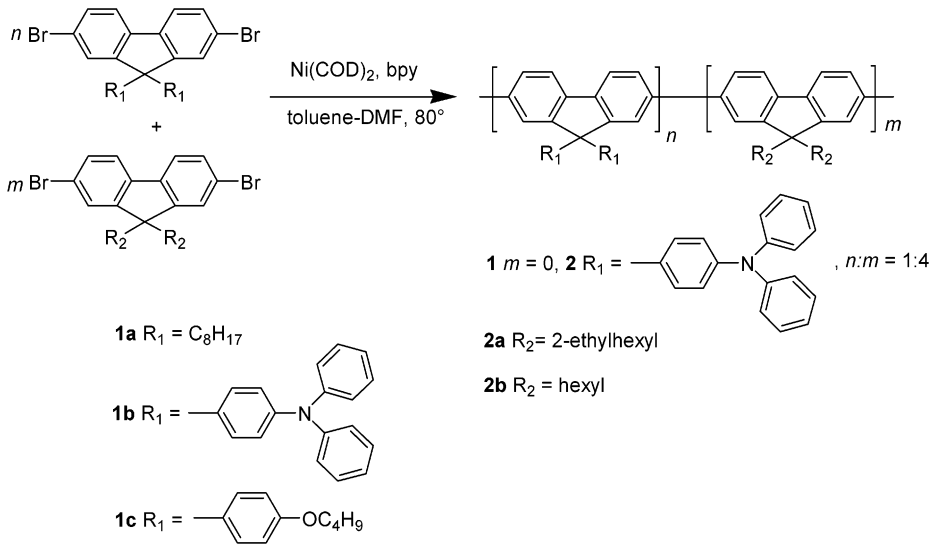

different chromophores have been used to improve charge transport[20] or to tune the emission color.[21] Moreover, the liquid-crystalline order of some PFs has opened the way to fabricate blue polarized electroluminescent devices.[22]

In conjugated materials, the molecular architecture strongly influences the supramolecular organization, which leads to specific morphologies in the solid state. The resulting microscopic structure of the films is of paramount importance since it impacts the optoelectronic properties.[13,23] The chain packing resulting for example from self-assembly processes and the corresponding interchain interactions influence the solid-state luminescence; several strategies can be used to optimize packing for light-emitting applications.[24]

Here, we report on a study of the relationship between the luminescence properties and the microscopic morphologies in thin deposits of homopolymers or copolymers built from differently substituted fluorenes (see Scheme 1). To establish the nature of the microscopic morphologies, we used tapping-mode atomic force microscopy (TM-AFM), which allows one to explore and image the topography (and other properties, via phase imaging) of the surface, with lateral and vertical resolution around 1 and 0.1 nm, respectively. To understand the AFM results in terms of supramolecular organization, comparisons were made with the results of molecular mechanics calculations carried out on single chains and on stacks of a few chains to determine the packing of the molecules as a function of the substitution pattern. Since packing is expected to strongly affect the optical properties, we also studied the solid-state photoluminescence of the films, which determines the potentiality of the materials for use in LEDs. A strong correlation is found between the luminescence properties, the morphological characteristics, and the macromolecular architecture (in particular, the substitution patterns).

Experimental Section

Synthesis. Polymer **1a**[25] (average chain length of 8 units) and polymer **1b**[19] (average chain length of 14 units) were synthesized as previously published. The other polymers and copolymers were prepared by coupling of the appropriate dihalo monomers with nickel(0). The synthesis of polymer **1c** is given by way of example.

A solution of $Ni(COD)_2$ (496 mg, 1.80 mmol), 2,2'-bipyridine (282 mg, 1.80 mmol), and 1-5 cyclooctadienyl (0.195 mg, 1.80 mmol) in dry DMF (10 mL) was heated at 75 °C for 30 min under an argon atmosphere. A solution of 2,7-dibromo-9,9-di-(4-butoxyphenyl)fluorene (533 mg, 0.86 mmol) in dry toluene (25 mL) was added and the mixture was heated at 75 °C for 48 h. The mixture was then poured into a methanol/HCl (2:1) mixture. The crude product was collected, dissolved in $CHCl_3$, and then reprecipitated from methanol/acetone (4:1). Residual impurities were removed by extraction with acetone in a Soxhlet apparatus to give the polymer **1c** (342 mg, 86%). GPC (toluene) M_n = 12940 g/mol; M_w = 26390 g/mol. D = 2.0 (PS standard). ^{1}H NMR (300 MHz, $CDCl_3$): 0.95 (t, 6H, CH_3), 1.42 (m, 4H, γ-CH_2), 1.7 (q, 4H, β-CH2), 3.88 (t, 4H, α-CH_2), 6.73 (d, 4H, H-a), 7.13 (d, 4H, H-b), 7.5 (m, 4H, H-c,d), 7.75 (d, 2H, H-e). ^{13}C NMR (125 MHz, $CDCl_3$): 13.79 (CH_3), 19.25 (CH_2), 31.40 (CH_2), 64.40 (C, fluorene-9), 67.63 (CH_2), 114.23 (CH), 120.29 (CH), 124.71 (CH), 126.61(CH), 129.21 (CH), 137.84 (C), 136.41 (C), 138.81 (C), 140.85 (C), 152.86 (C), 157.99 (C). UV absorption: λ_{max} ($CHCl_3$): 291, 401. Fluorescence: ($CHCl_3$) 420, 443 nm, (film) 457 nm.

Copolymer **2a** was obtained in 88% yield by reaction of a 4:1 mixture of 9,9-bis(4′-diphenylaminophenyl)fluorene and 2,7-dibromo-9,9-bis(2′-ethylhexyl)fluorene by the same procedure. GPC (THF, PPP standard, UV detection): M_n = 48950 g/mol, D = 2.0 (UV 388 nm), (THF, PPP standard, UV detection): M_n = 30200 g/mol, D = 2.1. ^{1}H NMR (300 MHz, $C_2D_2Cl_2$): 0.2−1.3 (m, 30 H, alkyl-H), 2.0 (m, 4H, alkyl-H), 6.6−7.3 (m, 14 H, TPA-H), 7.3−8.2 (m, 12H, fluorene-H). ^{13}C NMR (125 MHz, $C_2D_2Cl_2$): 10.74 (CH_3), 14.42 (CH_3), 23.08 (CH_2), 27.48 (CH_2), 28.58 (CH_2), 34.36 (CH_2), 34.98 (CH), 55.28 (C, fluorene-9), 120.12 (CH), 123.113 (CH), 124.65 (CH), 126.38 (CH), 129.54 (CH), 140.35 (C), 147.76 (C), 151.42 (C). UV

(20) Redecker, M.; Bradley, D. D. C.; Inbasekaran, M.; Wu, W. W.; Woo, E. P. *Adv. Mater.* **1999**, *11*, 241.
(21) Donat-Bouillut, A.; Lévesque, I.; Tao, Y.; D'Ioro, M.; Beaupré S.; Blondin, P.; Ranger, M.; Bouchard, J.; Leclerc, M. *Chem. Mater.* **2000**, *12*, 1931.
(22) Grell, M.; Knoll, W.; Lupo, D.; Meisel, A.; Miteva, T.; Neher, D.; Nothofer, H.-G.; Scherf, U.; Yasuda, A. *Adv. Mater.* **1999**, *11*, 671.
(23) Cadby, A. J.; Lane, P. A.; Mellor, H.; Martin, S. J.; Grell, M.; Giebeler, C.; Bradley, D. D. C. *Phys. Rev. B* **2000**, *62*, 15604.
(24) Cornil, J.; Beljonne, D.; Calbert, J.-P.; Brédas, J. L. *Adv. Mater.* **2001**, *13*, 1053.
(25) Marsitzky, D.; Klapper, M.; Müllen, K. *Macromolecules* **1999**, *32*, 8685.

absorption ($CHCl_3$): λ_{max}: 327, 395 nm. Fluorescence ($\lambda_{exc.}$ = 380 nm): 417, 439 nm ($CHCl_3$), 422, 446 nm (film).

Copolymer **2b** was obtained by the same procedure using a 4:1 mixture of 9,9-bis(4′-diphenylaminophenyl)fluorene and 2,7-dibromo-9,9-dihexylfluorene. (THF, PPP standard, UV detection): M_n = 31120 g/mol, D = 2.4.

Molecular Modeling. Molecular mechanics calculations were performed using the Cerius[2] package by Accelrys. We used the PCFF as the force field[26,27] as it has been validated previously for this type of system.[28] The long-range nonbonded interactions are calculated using the Spline method, with spline-on and spline-off parameters set to 11.0 and 14.0 Å, respectively. A conformer search was performed to obtain the most stable monomer geometry. Stacks of two to four oligomer molecules (from hexamers to decamers) were built. In the first step, the evolution of the total energy of the system was followed by allowing the substituents to move while keeping a constant distance between the backbones; several starting geometries and distances between backbones were tested. In the second step, equilibrium distances between the chains were obtained by minimization of the energy, while allowing the distance between the chains to evolve and the substituents to rotate. The Zoa v2.0 software was used for visualization and data presentation.[29]

Sample Preparation. For AFM investigations, all the samples were prepared in the same way: thin deposits were made by solvent-casting on freshly cleaved muscovite mica substrates from dilute solutions (from 0.05 to 0.1 mg/mL); the solvent (chosen to be a good solvent for the polymers, such as tetrahydrofuran or toluene) was evaporated slowly at room temperature in a solvent-saturated atmosphere.

Atomic Force Microscopy. Tapping-mode atomic force microscopy was performed with a Nanoscope IIIa microscope from Digital Instruments (operating in air, 25 °C). The instrument is equipped with the Extender Electronics Module to provide simultaneously height and phase cartography. Microfabricated silicon cantilevers were used with a spring constant of ~30 $N \cdot m^{-1}$. Images of different areas of the samples were collected with the maximum available number of pixels (512) in each direction. The Nanoscope image processing software was used for image analysis.

Photoluminescence Properties. The solid-state photoluminescence spectra of solution (in chloroform) and thin films on quartz substrates were obtained with a SPEX Fluorlog II (212) spectrometer equipped with a xenon lamp as the light source.

Results and Discussion

The study of the microscopic morphology of thin deposits of poly(9,9-dioctylfluorene) (PDOF **1a**, see Scheme 1) reveals the presence of fibrillar structures, that is, one-dimensional objects with a typical width of a few nm and length of several hundreds of nanometers to several micrometers. The fibrils are seen in Figure 1a as long bright objects, the mica substrate appearing dark; their measured height and width are 2.0 ± 0.2 and 8 ± 1 nm, respectively (thus displaying a ribbonlike shape). The image shows that the fibrils are straight (sometimes parallel to each other), suggesting a very regular packing of the molecules. This fibrillar morphology appears throughout the whole sample and can be reproduced independently of the solvent and the substrate used; it is thus the result of intrinsic self-assembly properties of the chains. The width of the ribbons (8 nm) is very close to the length of the fully extended molecule (including end caps) as calculated by molecular modeling (7.6 nm); the height is consistent with the substituents pointing nearly perpendicular to the substrate plane.

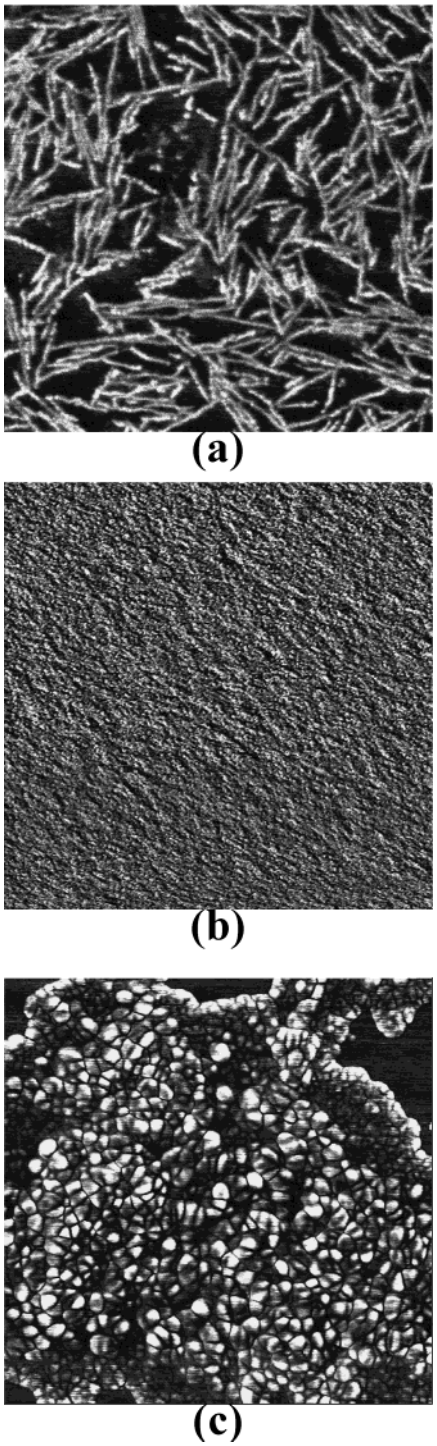

Figure 1. TM-AFM 1.0 × 1.0 μm^2 phase images of thin deposits on mica substrates of (a) PDOF **1a**, (b) PTPAF **1b**, and (c) **1c**.

These results suggest the following model for the assembly of the chains: the "ribbons" are stacks of conjugated chains, planar and parallel to each other, with the stacking direction parallel to the substrate plane and the substituents perpendicular to the stacking direction (see sketch in Figure 2c). Molecular mechanics

(26) Sun, H. *Macromolecules* **1995**, *28*, 701.
(27) Sun, H. *J. Comput. Chem.* **1994**, *15*, 752.
(28) Leclère, Ph.; Hennebicq, E.; Calderone, A.; Brocorens, P.; Grimsdale, A. C.; Müllen, K.; Brédas, J. L.; Lazzaroni, R. *Prog. Polym. Sci.* **2003**, *28*, 55.
(29) Zoa v.2.5, J. P. Calbert, Service de Chimie des Matériaux Nouveaux, Université de Mons-Hainaut, Mons, Belgium; http://zoa.freeservers.com.

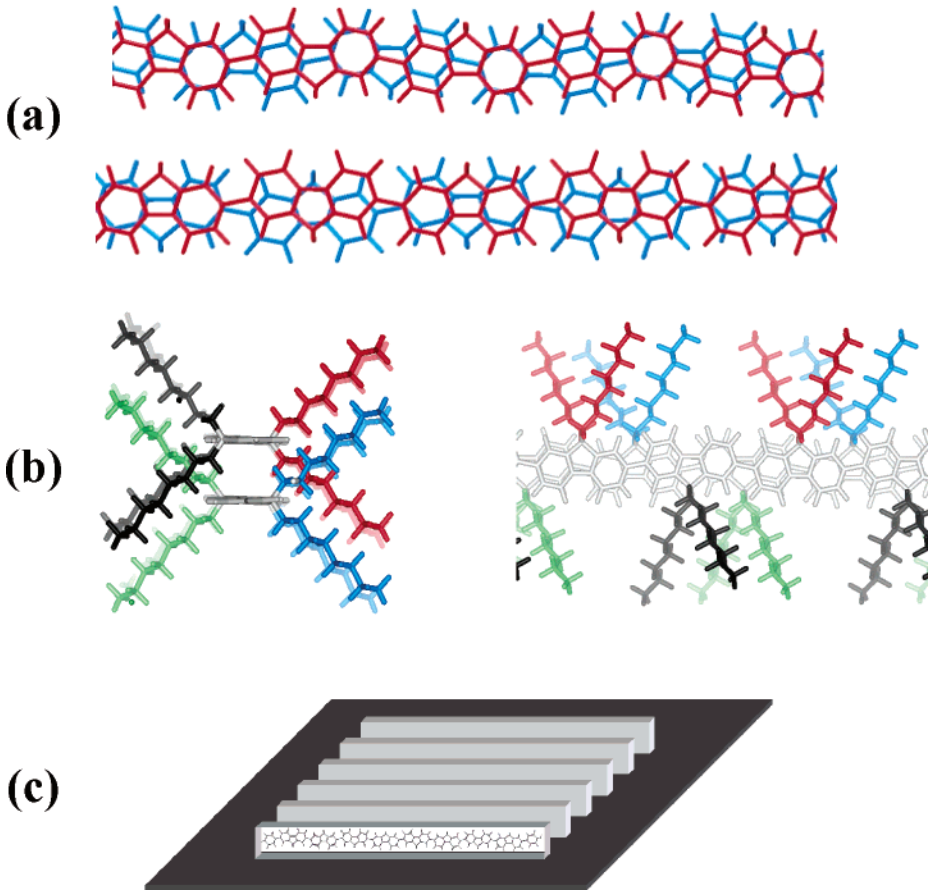

Figure 2. Molecular modeling of the assembly of polyfluorene, PF, chains ("stick" representation): (a) "shifted" (top) and "flipped" (bottom) starting configurations (represented without substituents); (b) most stable packing of two chains of di-octyl-substituted PF: views with PF chains perpendicular (left) and parallel (right) to the view; (c) sketch of the packing of molecules into a fibril on the substrate (black); for the sake of clarity, the substituents are not represented.

calculations confirm the tendency of the molecules to form this type of stack (see below), the driving force for such a supramolecular organization being the $\pi-\pi$ interactions between adjacent chains. This fibrillar morphology is a typical signature of the self-assembly of planar conjugated polymer chains; it has been observed in a number of systems including for example poly(3-alkylthiophene),[30] poly(*p*-phenylene ethynylene),[31−33] and poly(9,9-dialkylfluorene).[28,34,35] Near-field scanning optical microscopy studies on pristine films of poly(9,9-dialkylfluorene)[35,36] have demonstrated the presence of similar fibrillar structures and clearly shown that the polymer chains are perpendicular to the ribbon axis, in agreement with the model proposed here.

To evaluate the impact of substitution on the supramolecular organization, we investigate thin deposits of PFs with aryl-based substituents: poly(9,9-ditriphenylaminefluorene) (PTPAF) (**1b**) and poly(9,9-di-4-butoxyphenylfluorene) (**1c**). Note that, in both cases, the substituents are bulky. PTPAF (**1b**) is of particular interest because triphenylamine has an ionization potential between those of PDOF and ITO, which acts as the anode in LEDs, and improves hole injection in such devices.[19] Figure 1b illustrates the microscopic morphology of thin deposits of PTPAF and shows a uniform, smooth film; the surface is very flat (the value of the RMS roughness being 0.3 nm over 1 μm^2), without any specific structure. The microscopic structure of a thin deposit of **1c** is shown in Figure 1c: the phase image, which is more sensitive to local variations in tip−sample interactions (for example, topographical and/or mechanical variations), presents a granular morphology.

Since the same conditions of preparation and imaging were used for **1b** and **1c** as for the PDOF samples, and the polymers (**1a**, **1b**, **1c**) have similar, low degrees of polymerization, the differences in microscopic morphology can be attributed to the differences in substitution. Octyl-substitution of the polyfluorene chains allows for a close packing of the conjugated segments ("π-stacking"), while the steric hindrance due to the bulkier aryl-based substituents prevents this type of stacking. To confirm this hypothesis, we performed molecular mechanics calculations on stacks of a few chains (from two to four). Note that the conjugated backbones are taken to be coplanar, as expected in the solid state. Two initial configurations have been mainly considered, namely, a

(30) Merlo, J. A.; Frisbie, C. D. *J. Polym. Sci., Part B: Polym. Phys.* **2003**, *41*, 2674.
(31) Samori, P.; Francke, V.; Müllen, K.; Rabe, J. P. *Thin Solid Films* **1998**, *336*, 13.
(32) Samori, P.; Francke, V.; Mangel, T.; Müllen, K.; Rabe, J. P. *Opt. Mater.* **1998**, *9*, 390.
(33) Bunz, U. H. F.; Enkelmann, V.; Kloppenburg, L.; Jones, D.; Shimizu, K. D.; Claridge, J. B.; zur Loye, H.-C.; Lieser, G. *Chem. Mater.* **1999**, *11*, 1416.
(34) Chappell, J.; Lidzey, D. G.; Jukes, P. C.; Higgins, A. M.; Thompson, R. L.; O'Connor S.; Grizzi, I.; Fletcher, R.; O'Brien, J.; Geoghegan, M.; Jones, R. A. L. *Nature Mater.* **2003**, *2*, 616.
(35) Teetsov, J. A.; Vanden Bout, D. A. *J. Am. Chem. Soc.* **2001**, *123*, 3605.
(36) Teetsov, J. A.; Vanden Bout, D. A. *Langmuir* **2002**, *18*, 897.

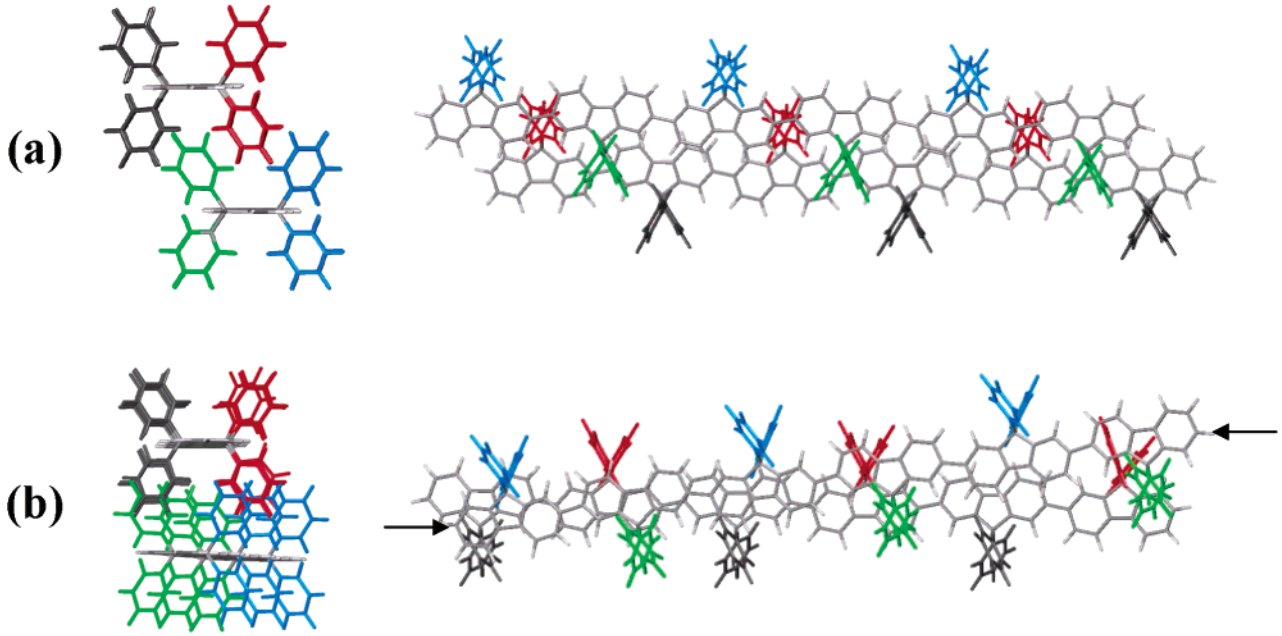

Figure 3. Molecular modeling of the assembly of phenyl-substituted PF chains ("stick" representation). Optimal configurations obtained from (a) the "shifted" starting configuration and (b) the "flipped" starting configuration (views with PF chains perpendicular (left) and parallel (right) to the view).

"flipped" configuration and a "shifted" configuration. These configurations have been chosen since they yield the smallest steric hindrance and are therefore more likely to lead to a close packing of the PF chains. In the "shifted" configuration (Figure 2a top), adjacent PF chains are translated relative to one another along the chain axis by half a period; in this way, the side chains on one oligomer are located in front of the interunit bond of the other oligomer. In the "flipped" configuration, the monomer units of neighboring PF chains are superimposed, but the bridging sites (that carry the substituents) point in opposite directions.

In the first step of a given simulation, the intermolecular separation was kept fixed while the side groups were allowed to relax and reach an equilibrium configuration; the distance between chains was varied between 4.0 and 7.0 Å. In doing so, insight is gained into the way the side groups react to steric hindrance. In the second step, the partially optimized configurations were used as starting conformations in another optimization procedure in which the interchain distance is allowed to vary. The alkyl side chains were considered to be in a planar zigzag conformation since this is most likely to allow close packing of PF chains. Stable, regular assemblies have been obtained for "Y"-shaped fluorene units, that is, the conformation in which the second C−C bond of each alkyl group is nearby parallel to the fluorene plane; see Figure 2b. The results indicate that stable assemblies with "Y"-shaped monomer units can be obtained in both "flipped" and "shifted" configurations with equilibrium distances between chains of about 5.0 Å. The results are illustrated in Figure 2b when starting from the "shifted" configuration (the most stable one); the structures highlight the cofacial configuration of the PF chains and underline the possibility for the π molecular orbitals of adjacent chains to overlap significantly. This confirms that, provided the alkyl substituents adopt a suitable conformation, close packing of the PF chains can be achieved. This behavior has been confirmed for larger systems, that is, stacks of three and four chains. Extension of this π-stacking to a large number of chains leads to a fibrillar morphology, as sketched in Figure 2c, consistent with the AFM results. We note that, for the fibrils a few hundred nanometers long observed by AFM, considering that the equilibrium distance between chains is about 5 Å, the number of molecules in a given fibril is over 1000.

Similar calculations were performed on di-phenyl-substituted PF, as a model system for the aryl-substituted polymers studied experimentally. The results show that the system strongly stabilizes when the distance between the PF backbones is increased from 4.0 to 7.0 Å. Despite an extensive conformational search, we have found no stable configuration in which the distance between two adjacent π-backbones comes down to about 5 Å, in contrast to the case of the alkyl-substituted polymer. Here, the chains tend to move away and drift sideways from each other due to the steric repulsion among the bulky phenyl substituents. This is illustrated in Figure 3a, which shows the most stable configuration obtained after minimization from the starting "shifted" configuration: the equilibrium distance between chains is found to be near 8.0 Å (PF backbones are shown perpendicular (left) and parallel (right) to the view). The results for the "flipped" configuration are shown in Figure 3b: a nonparallel arrangement of the PF chains is found (see the arrows pointing at the two ends of one of the chains) and the equilibrium distance is between 7.5 and 8.0 Å. Thus, in the case of phenyl substituents, the PF chains cannot pack closely in a cofacial way. The calculated equilibrium distances between adjacent backbones are much larger than the values obtained in the case of di-octyl-substituted oligofluorenes; they are clearly inconsistent with the formation of regular, compact π-stacks; that is, the interchain distance is too large for significant overlap of π-orbitals to occur. Again, this trend was confirmed in the calculations on the three-chain and

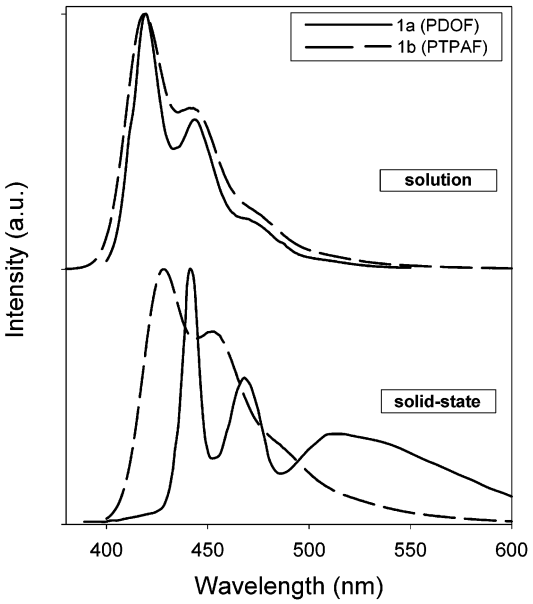

Figure 4. Photoluminescence spectra of PDOF **1a** (full line) and PTPAF **1b** (dashed line): (top) solution spectra (in chloroform); (bottom) solid-state spectra.

four-chain clusters. Since polymers **1b** and **1c** have substituents that are phenyl-based and are even bulkier, it is expected that in the solid state they would form assemblies of molecules with no long-range organization and therefore nontextured microscopic morphologies.

To study the impact of the microscopic morphology on the optical properties, the photoluminescence spectra of **1a** (PDOF) and **1b** (PTPAF) are studied. In solution (in chloroform, in which the compounds are molecularly dissolved), the two polymers produce essentially identical spectra with well-defined vibronic progression (Figure 4 top): the maxima of emission are located at 419 nm (2.96 eV), 442 nm (2.81 eV), and a band around 470 nm. The solid-state fluorescence spectra of **1a** and **1b** are markedly different, as illustrated in Figure 4 bottom: PDOF **1a** shows a vibronic progression with two well-defined maxima at 442 nm (2.81 eV) and 468 nm (2.65 eV), along with an additional broad band above 500 nm. The large red shift (compared to solution spectrum) and the broad band above 500 nm have been initially attributed to emission from excimers or aggregated chains;[12] more recently, the band in the 500−550-nm region has been shown to be due to emission from fluorenone-like defects due to oxidative (photo- or electro-) degradation of the film.[13,37−39] In contrast, the fluorescence of PTPAF **1b** closely resembles its solution spectrum, with maxima at 428 nm (2.90 eV) and 452 nm (2.74 eV) and no peak in the low-energy region. The same is true for the solid-state emission spectrum of **1c** that shows a peak at 457 nm (2.71 eV, pure blue emission), with no emission in the low-energy region. Photoluminescence spectra in solution are almost identical for the two compounds **1a** and **1b**; this indicates that the differences in the solid-state spectra originate from differences in (i) the chemical stability of the fluorene moieties vs oxidation in the solid state and/or (ii) the microscopic structure of the films (i.e., the difference in packing). These two polymers are both made of di-substituted fluorene units, which are more stable to oxidation than monosubstituted fluorene polymers.[13] It would be very difficult to determine the amount of fluorenone defects in the thin films studied here. Although it has been proposed by Scherf et al. that the formation of fluorenone defects could be reduced in aryl-substituted PF compounds compared to alkyl-substituted ones,[38] we think that the microscopic morphology of the films plays an important role on the luminescence properties (as clearly shown in copolymers having similar substituents but different morphologies, see below): the dense interchain packing in fibrils of **1a** promotes the fast migration of the excitons to emissive defect (fluorenone) sites, which leads to the green emission band (and to sites where nonradiative decay is possible, thus decreasing the luminescence efficiency[40]). For aryl-substituted PFs (**1b** and **1c**), however, there only occurs a very small red shift in solid-state fluorescence compared to the situation in solution, due to the fact that exciton migration is hindered and the fluorescence mostly arises from emission of single chromophores.

Another way to disturb the regular organization of conjugated polymer chains is to consider random or alternated copolymers. In this context, we have investigated two PFs obtained by random copolymerization: di-triphenylaminefluorene copolymerized in a 1:4 ratio with di-ethylhexylfluorene **2a** or with di-hexylfluorene **2b** (Scheme 1). Thin deposits of **2a** reveal uniform, smooth featureless films as shown in Figure 5a, with a rms roughness of only 0.6 nm. Such a low value indicates that these films are particularly flat; we did not observe any fibril (or organized structures) for this system. Note that films of the copolymer with the same chemical structure as **2a** but with a 1:1 ratio of the comonomers also show a smooth microscopic morphology, without any specific structure. Molecular modeling calculations indicate that ethylhexyl-substituted PF chains cannot close pack because of steric hindrance among substituents; instead the conjugated backbones of adjacent chains tend to move away from each other, with distances between adjacent backbones larger than 7.0 Å. The fact that polymer **2a** exhibits no fibrillar morphology is thus consistent with the fact that both homopolymers of di-triphenylaminefluorene and di-ethyhexylfluorene do not allow for a close packing of the chains.

The microscopic morphology of thin deposits of **2b** is shown in Figure 5b: we distinguish three levels of contrast, corresponding to the substrate (in dark) and to thin "wires" (in gray), which join brighter, flat areas. We find from an image analysis that the "wires" have relatively constant widths, between 20 and 30 nm, and a constant height of about 2.0 nm while the connected bright structures have varying heights (between 4.0 and 6.0 nm) and lateral dimensions (from few tens to few hundreds of nanometers). The large structures may

(37) Zojer, E.; Pogantsch, A.; Hennebicq, E.; Beljonne, D.; Brédas, J. L.; Scandiucci de Freitas, P.; Scherf, U.; List, E. J. W. *J. Chem. Phys.* **2002**, *117*, 6794.
(38) List, E. J. W.; Guentner, R.; Scandiucci de Freitas, P.; Scherf, U. *Adv. Mater.* **2002**, *14*, 373.
(39) Romaner, L.; Pogantsch, A.; Scandiucci de Freitas, P.; Scherf, U.; Gaal, M.; Zojer, E.; List, E. J. W. *Adv. Funct. Mater.* **2003**, *13*, 597.
(40) Grimsdale, A. C.; Leclère, Ph.; Lazzaroni, R.; Mackenzie, J. D.; Murphy, C.; Setayesh, S.; Silva, C.; Friend, R. H.; Müllen, K. *Adv. Funct. Mater.* **2002**, *12*, 729.

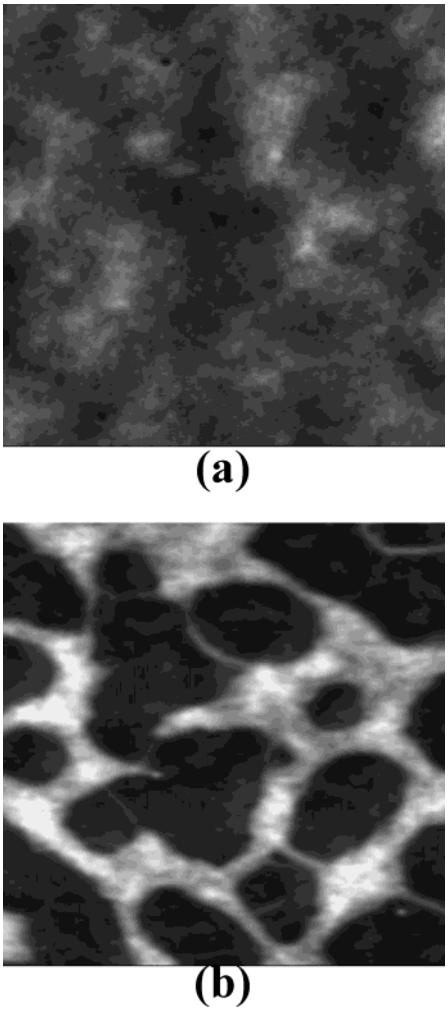

Figure 5. TM-AFM height images of thin deposits on mica of (a) **2a** ($2.0 \times 2.0\ \mu m^2$) and (b) **2b** ($1.0 \times 1.0\ \mu m^2$). The vertical gray scale is 5.0 and 7.0 nm, respectively.

originate from dewetting, while the constant dimensions of the wires and their aspect ratio is reminiscent of the fibrillar morphology. We believe that these objects are an indication that some long-range organization of the chains can occur. This is consistent with the fact that the chains are rich in di-hexylfluorene units (4 times more abundant than di-triphenylamine-fluorene units). It is likely that relatively long sequences of di-hexylfluorene units are present along the chains; such sequences could pack locally with corresponding segments in neighboring chains, as occurs in PDOF, thereby giving rise to organized structures (the wires). However, the presence of TPA-substituted units tends to disrupt close packing and long-range organization and leads to the prevalence of amorphous structures (the connected bright structures).

The same approach to control microscopic morphology via molecular architecture has been recently applied to tetraalkyl-indenofluorene-based polymers: it has been reported[40] that ethylhexyl-substituted polyindenofluorenes (PTEHIF) do not show any fibrillar morphology, while tetraoctyl-substituted polyindenofluorenes (PTOIF) form fibrils similar to those seen here for PDOF. In random PTEHIF−PTOIF copolymers, the ratio between the two monomers controls the microscopic morphologies of thin deposits: a 9:1 ratio (PTOIF−PTEHIF) leads to fibrils while a 1:9 ratio leads to nontextured, disordered morphologies.

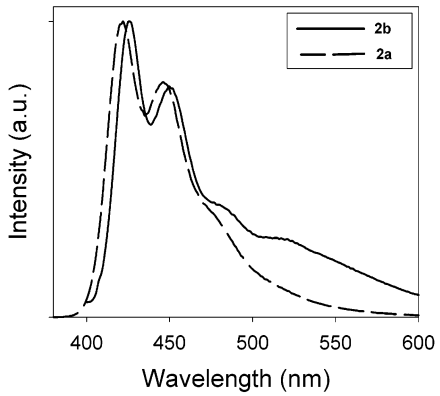

Figure 6. Solid-state photoluminescence spectra of **2a** (dashed line) and **2b** (full line).

The emission spectrum of **2a** in solution (in chloroform) shows two bands appearing at 417 and 439 nm (2.97 and 2.82 eV, respectively); the solid-state spectrum closely resembles the one in solution, with the bands slightly shifted to 422 and 446 nm (2.94 and 2.78 eV, respectively, see Figure 6). The absence of a significant red shift in fluorescence is consistent with a nonorganized microscopic structure (smooth film), due to a molecular architecture with crowded substituents. Polymer **2b** has a similar emission spectrum in solution than **2a** and exhibits the same type of solid-state spectrum as **2a** (Figure 6) for the two major peaks; however, it also shows a long wavelength band extending into the green, which is not present for polymer **2a**. Most probably, the difference in stability toward oxidation does not play a major role (since the only difference between the two systems is the structure of the alkyl substituents -hexyl vs ethylhexyl-, with identical aryl content). Therefore, the long-wavelength peak is attributed to the possibility, within the "wires", of facile migration of excitons to emissive defect sites arising from dense local packing and interactions among chains.

Synopsis

We have shown that the microscopic morphology of thin deposits of fluorene polymers and copolymers is strongly correlated with their molecular architecture; the substitution patterns are of prime importance in determining whether organized or nonorganized assemblies are obtained. Linear alkyl substituents allow for a close packing of the molecules into nanoribbons. Bulky substituents (aryl-based or branched alkyl chains such as ethylhexyl) lead to nonorganized deposits because of the steric hindrance between the chains; the steric interactions tend to separate the conjugated backbones beyond the distance where π-stacking can be a driving force for the organization into nanoribbons.

The competition between steric hindrance and π-stacking is of prime importance in defining the optoelectronic properties in these materials. The photoluminescence properties are highly dependent on the morphology: organized structures lead to significant long wavelength emission in the green while nonorganized structures (granular and smooth films) caused by bulky substituents retain pure blue emission, which can be useful for light-emitting applications.

Acknowledgment. The collaboration between Mons and Mainz is conducted in the framework of the Inter-University Attraction Pole Program (PAI V/3) of the Belgian Federal Government and the European Science Foundation "*Structuring, Manipulation, Analysis and Reactive Transformation of Nanostructures* (SMARTON)" program. Research in Mons is partly supported by the European Commission, the Government of the Region of Wallonia (Phasing Out − Hainaut), and the Belgian National Fund for Scientific Research FNRS/FRFC. The work at Georgia Tech is partly supported by the National Science Foundation (CHE-0071889). E.H is Aspirante de Recherches du F.N.R.S. M.S. acknowledges F.R.I.A. for a doctoral scholarship. C.E. acknowledges the Fondation Universitaire David et Alice Van Buuren for financial assistance.

CM0349452